AIR FORCE INSTITUTE OF TECHNOLOGY

AIR UNIVERSITY
UNITED STATES AIR FORCE

SCHOOL OF ENGINEERING

WRIGHT-PATTERSON AIR FORCE BASE, OHIO

AF-WP-O-MAY 62 3,500

A CORRELATION STUDY OF

PLASMA DIAGNOSTIC TECHNIQUES

Lt. Robert R. Murfitt

GNE/Phys/62-11

A CORRELATION STUDY OF
PLASMA DIAGNOSTIC TECHNIQUES

THESIS

Presented to the Faculty of the School of Engineering of
the Institute of Technology (Air University)
in Partial Fulfillment of the
Requirements for the Degree of
Master of Science

By

Robert Roscoe Murfitt

1/Lt. USAF

Graduate Nuclear Engineering

May 1962

Preface

This report is the result of an attempted correlation between microwave measurements and spherical Langmuir probe measurements in a mercury plasma. We hoped to verify the electron velocity distribution function which we obtained with spherical probes by measuring the conductivity ratio of the plasma with microwaves. Although the lack of sufficient time and the need for redesigning the equipment prevented us from obtaining the desired correlation, I believe that further work in this area will be successful.

I wish to thank Dr. G. Medicus and Mr. W. Eppers for helping me to understand the theory of the spherical probe and the cylindrical microwave cavity, and Mr. F. Ruff and Mr. W. I. Borodatschew for constructing the equipment which I used.

Robert R. Murfitt

Contents

Contents

List of Figures

List of Tables

List of Symbols

B - Slope of the plot of power ratio vs frequency difference squared.

cm - Centimeters.

db - Decibels.

e - Charge of an electron.

f - Electron velocity distribution function.

F - Effective electrode area of a spherical probe.

Hg - Mercury.

i - Probe current.

k - Boltzmann's constant

ma - Milliamperes.

mm - Millimeters.

m - Mass of an electron.

ν_c - Frequency of electron collision.

σ_i - Imaginary part of the conductivity.

σ_r - Real part of the conductivity.

t - Characteristic velocity of the electrons.

T - Electron temperature.

v - Velocity of an electron.

V - Probe voltage.

vs - Versus.

ω - Microwave frequency in radians.

Abstract

The ratio of the real to the imaginary conductivity of a neutral plasma can be determined in several ways. If the velocity distribution and the collision frequency of the electrons in the plasma are known, this conductivity ratio can be calculated; and if the plasma is confined in a microwave cavity, measurements of the power which enters and emerges from the cavity can also be used to calculate this ratio. This gives two independent methods of calculating the same quantity, the conductivity ratio.

A cylindrical microwave cavity that could be filled with a mercury plasma was designed and built in such a way that spherical Langmuir probes could be inserted into the plasma in the cavity. The spherical probes were used in an attempt to determine the velocity distribution function of the electrons, but the lack of results from the probes made it necessary to assume a Half-Maxwellian distribution function existed within the cavity. Microwave measurements of the conductivity ratio agreed quite well with the conductivity ratio which was calculated from the assumed distribution function, but the large standard deviation in the microwave measurements indicates that further refinements in design are necessary. The probability of collision of the electrons in mercury vapor is such that the effect of the electron velocity distribution function on the conductivity ratio is minimized, and the redesign of the equipment for use with a rare gas plasma is necessary before the microwave measurement of the conductivity ratio can be used

to confirm that a given distribution function exists in the plasma.

GNE/Phys/62-11

A CORRELATION STUDY OF PLASMA DIAGNOSTIC TECHNIQUES

I. Introduction

This study was undertaken as the first project in a correlation study in plasma diagnostics by the Electron Technology Laboratory at Wright-Patterson Air Force Base, Ohio. The Electron Technology Laboratory had carried out extensive work with Langmuir probes in neutral plasmas of various gases, but a method of confirming the electron velocity distributions which were derived from the probe studies was desired. An independent method of determining the electron velocity distribution would not only serve as a check on the Langmuir probe studies, but also determine under what conditions of the plasma the probe could be used as an effective diagnostic tool.

A considerable amount of work had been carried out at the Massachusetts Institute of Technology using microwaves as a plasma diagnostic tool. It was decided that a correlation study would be attempted using the spherical Langmuir probe and simultaneous microwave measurements.

The only previous work of this type that had been attempted was by R. C. Jones at the United States Naval Research Laboratory (See Ref 6). The apparatus which was used by Jones contained the plasma in a glass envelope. Probes were inserted into the plasma and microwave transmission measurements were made by beaming the microwaves

through the plasma envelope which was placed between two microwave horns. The plasma was formed in Jones' experiment by microwave excitation.

In the correlation study which was undertaken for this thesis a mercury plasma was formed by a heated cathode and inclosed in a nickel plated, cylindrical, microwave cavity. The cylindrical shape was chosen since the derivation of the microwave equations for this geometry had been carried out previously by S. C. Brown, et al., at the Massachusetts Institute of Technology and published as a series of articles in the Journal of Applied Physics (See Ref 10; Ref 11; Ref 12; Ref 4). The cavity was nickel plated to resist the corrosive effect of mercury. A mercury plasma was chosen for these initial measurements since it is easy to produce, and the Electron Technology Laboratory had previously used mercury plasmas in much of their probe diagnostics. As will be pointed out in later portions of this work, the choice of a mercury plasma was unfortunate and severely limited the results which were attainable.

This report will first discuss the theoretical behavior of a microwave cavity which contains a neutral plasma. Then the voltage and current relationship of a spherical Langmuir probe in a region containing a plasma will be discussed briefly. The type of microwave cavity and probe which was used in this study and the procedure which was followed are then discussed, and the method of processing the data which was taken is then covered. A discussion of the results which were obtained and recommendations for further study along these lines

conclude the report.

II. Theory

The utility of a microwave cavity as a plasma diagnostic tool results from the equation

$$\frac{\sigma_r}{\sigma_i} = - \frac{\int_0^\infty \frac{(\nu_c/\omega)\, v^3\, df}{1 + (\nu_c/\omega)^2}}{\int_0^\infty \frac{v^3\, df}{1 + (\nu_c/\omega)^2}} \qquad (1)$$

(Ref 7:316) where σ_r and σ_i are the real and imaginary parts of the complex conductivity of the cavity, ν_c is the collision frequency of the electrons, v is the electron velocity, f is the electron distribution function, and ω is the radian frequency of microwaves which are used for the measurements. The derivation of this equation was carried out by H. Margenau (Ref 8:508).

Microwave Theory

The measurement of σ_r/σ_i by experimental means allows one to verify if a given electron distribution function exists within the cavity. This ratio was determined by the method outlined by L. Gould and S. C. Brown of the Massachusetts Institute of Technology (Ref :1053).

Microwave Circuitry. L. Gould and S. C. Brown analysed the microwave cavity by using the equivalent circuit shown in Fig. 1, where g_s is the conductance of the input line, g is the conductance of the empty cavity, g_n is the conductance which is reflected back into the cavity from the output line, g_d is the conductance of the plasma discharge, b is the susceptance of the cavity, and b_d is the susceptance of the

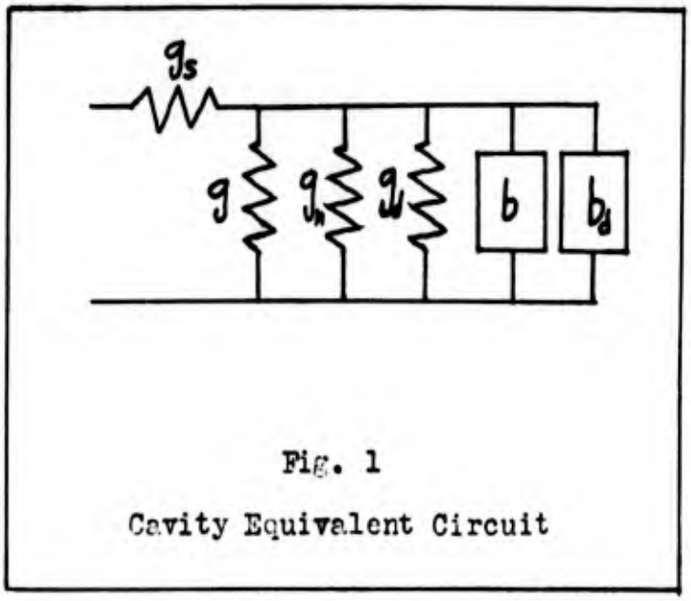

Fig. 1

Cavity Equivalent Circuit

plasma discharge. By defining

$$g_t = g + g_n + g_d \tag{2}$$

and

$$b_t = b + b_d \tag{3}$$

the impedance of the cavity is given by

$$Z = \frac{1}{g_s} + \frac{1}{(g_t + jb_t)} \tag{4}$$

Power Ratio. If the microwave power which enters the cavity is denoted by P_i, the power which is absorbed in the cavity by P_a, and the power which passes into the output line by P_t; the following equations relate P_t and P_i

$$P_a = P_i\left(1 - \left|\frac{Z-1}{Z+1}\right|^2\right) \tag{5}$$

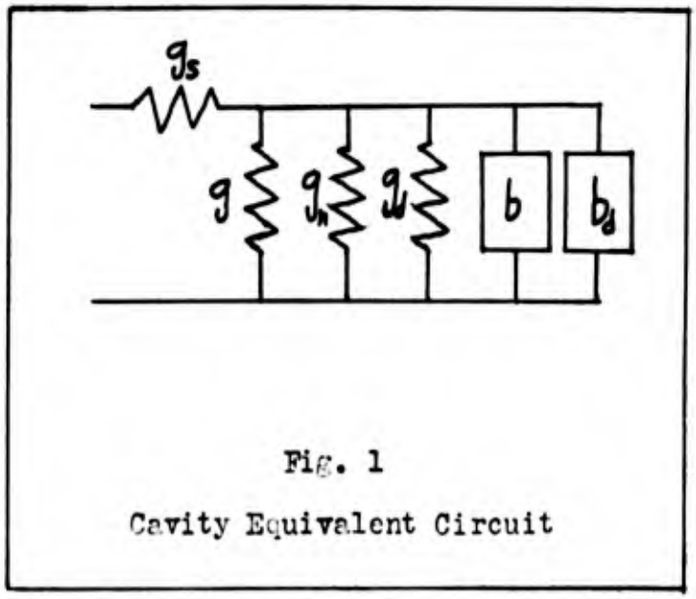

Fig. 1
Cavity Equivalent Circuit

plasma discharge. By defining

$$g_t = g + g_n + g_d \tag{2}$$

and

$$b_t = b + b_d \tag{3}$$

the impedance of the cavity is given by

$$Z = \frac{1}{g_s} + \frac{1}{(g_t + jb_t)} \tag{4}$$

Power Ratio. If the microwave power which enters the cavity is denoted by P_i, the power which is absorbed in the cavity by P_a, and the power which passes into the output line by P_t; the following equations relate P_t and P_i

$$P_a = P_i\left(1 - \left|\frac{Z-1}{Z+1}\right|^2\right) \tag{5}$$

$$\frac{P_a}{P_i} = \frac{4\left[(g_t^2 + b_t^2)/g_s + g_t\right]}{\left[\left(\frac{1}{g_s}+1\right)g_t+1\right]^2 + b_t^2\left(\frac{1}{g_s}+1\right)^2} \tag{6}$$

$$P_t = P_a\left(\frac{g_n}{g_t}\right)\frac{g_t/(g_t^2+b_t^2)}{\left[g_n/(g_t^2+b_t^2)+1/g_s\right]} \tag{7}$$

$$P_t = P_i\, 4g_n\left\{\left[\left(1/g_s+1\right)g_t+1\right]^2 + b_t^2\left(1/g_s+1\right)^2\right\}^{-1} \tag{8}$$

Since (Ref 12:1028)

$$b = \beta\left(\frac{\omega}{\omega_o} - \frac{\omega_o}{\omega}\right) \tag{9}$$

then

$$b_t = \beta\left(\frac{\omega}{\omega_o} - \frac{\omega_o}{\omega}\right) + b_d \tag{10}$$

but (Ref 4:1054) the approximation

$$b_d = -2\beta(\omega_o' - \omega_o)/\omega \tag{11}$$

holds, if the discharge perturbs the resonance frequency of the cavity only by a slight amount. This allows the approximation

$$b_t = 2\beta(\omega - \omega_o')/\omega \tag{12}$$

where β is the coupling coefficient between the cavity and the transmission line, ω_o' and ω_o are the resonance frequencies of the cavity with and without the plasma discharge, and ω is the microwave frequency which is used for the measurement.

Conductivity Ratio. If the quantity $2(\omega - \omega_o')$ is defined to equal a new variable, X, equations (8) and (12) can be combined to give

$$\frac{P_i 4 g_n}{P_t[(1/g_s+1)g_t+1]^2} = 1 + \frac{\beta^2 X^2 (1/g_s+1)^2}{\omega^2[(1/g_s+1)g_t+1]^2} = \gamma \qquad (13)$$

where γ is a new variable which is defined for convenience by the above equation.

If the new variable, γ, is plotted as a function of X^2, the square root of the reciprocal of the slope of the line is given by

$$\frac{\omega g_t}{\beta} + \frac{\omega}{\beta(1/g_s+1)} = \alpha \qquad (14)$$

where alpha is defined by the above equation for convenience. If the γ function is plotted with a plasma discharge in the cavity and again without a discharge, the difference in α will be caused by the change in g_t. This difference in g_t will be equal to g_d which gives

$$\Delta\alpha = \omega g_d/\beta \qquad (15)$$

From equation (11)

$$\beta = \frac{b_1 \omega}{2(\omega_o - \omega_o')} \qquad (16)$$

or

$$\frac{\Delta\alpha}{2(\omega_0-\omega_0')}=\frac{g_d}{b_d} \tag{17}$$

Since (Ref 12:1031)

$$\frac{\sigma_n}{\sigma_i}=\frac{g_d}{b_d} \tag{18}$$

the left hand side of equation (1) can be determined by measuring α and ω_0 with and without a plasma discharge in the cavity.

The plotting of γ vs X^2 is achieved from data which is obtained experimentally by the null method of Gould and Brown (Ref 4:1053). Equation (13) shows that $\gamma=1$ when $X=0$, therefore, γ can be plotted as a function of X^2 by measuring the ratio of the power which is incident into the cavity to the power which is transmitted from the cavity.

The above analysis, which was taken from L. C. Gould and S. C. Brown's article "Methods of Measuring the Properties of Ionized Gases at High Frequencies, IV. A Null Method of Measuring the Discharge Admittance." (Ref 4:1053), requires that the plasma does not disturb the electric field in the cavity, the electrons undergo only elastic collisions, the collision frequency of the electrons is much less than the microwave frequency which is used for the measurements, and the electron velocity distribution is uniform throughout the microwave cavity.

Slope Correction. When an attempt was made to apply the above theory, difficulty was encountered in measuring the power ratio at the exact point where $X=0$, which is at the exact resonance frequency of

the cavity. Therefore, the γ function was not exactly equal to one when the initial ratio of P_i/P_t was determined (See Chapter IV on experimental procedure). This error in the ratio of P_i/P_t introduced an error into the values of α which were later determined.

The equivalent circuit in Fig. 2 was used to analyse the error, where k is the gain in the incident power circuit and A is the variable gain in the transmitted power circuit. Since the traces on the oscilloscope, which are proportional to the power in each circuit, are superimposed before every reading

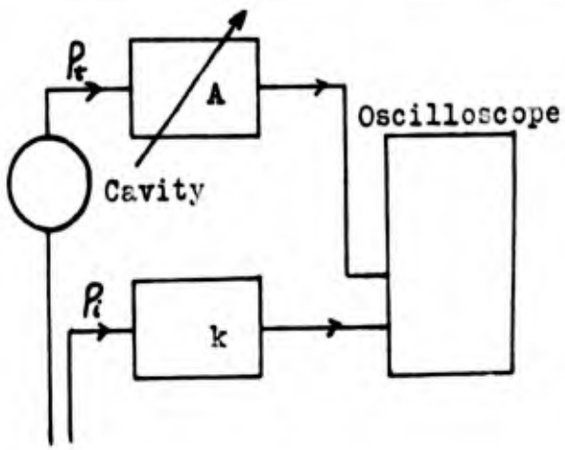

Fig. 2

Simplified Microwave Circuit

$$P_i k = P_t A \tag{19}$$

or

$$\frac{P_i}{P_t} = \frac{A}{k} \tag{20}$$

Equation (13) was simplified for analysis by inserting the two constants

$$C = 4g_n/[(1/g_s + 1)g_t + 1]^2 \tag{21}$$

$$B = \frac{\beta^2(\nu_{es}+1)^2}{\omega^2[(\nu_{es}+1)\nu_e+1]^2} \tag{22}$$

to give

$$\frac{P_i}{P_e}C = 1 + BX^2 \tag{23}$$

By substituting equation (20) into equation (23) and solving for A, the equation

$$A = \frac{k}{C} + \frac{Bk}{C}X^2 \tag{24}$$

is obtained. The experimental procedure which was used determined A as a function of X^2; therefore, the slope of the plot of A vs X^2 is Bk/C while

$$\alpha = \sqrt{\frac{1}{B}} \tag{25}$$

from the previous theory. By dividing the slope of the plot of A vs X^2 by the value of A at $X^2 = 0$, the value of B is obtained and the value of α can be determined from equation (25).

Probe Theory

The theory of the Langmuir probe will not be dealt with in detail since it is readily available in existing publications. L. B. Loeb (Ref 7:342) gives a derivation by M. J. Duryvesteyn (Ref 3:790) which shows that the second derivation of the probe current with respect to the probe voltage, when the probe is negative with respect to the plasma is given by

$$\frac{d^2i}{dV^2} = \frac{e^2F}{4m}\frac{1}{V}f\left(\sqrt{\frac{2eV}{m}}\right) \tag{26}$$

where e is the electronic charge, F is the effective electrode area of the probe, m is the mass of the electron, and f is the electron distribution function. From this equation it can be seen that the product of the second derivation of the probe current and the probe voltage gives a function which is proportional to the electron distribution function. If the second derivation of the probe current is determined as a function of the probe voltage, we are able to determine the form of the electron distribution function.

Second Derivative of Probe Current. If a small alternating potential of the form Asin(pt) is imposed upon the negative direct current potential, V, of probe, the probe current, i, can be expressed (Ref 7:345) by the series

$$\begin{aligned} i = {} & I(V) + A^2 I''(V) + A^4 I''''(V) + [A I'(V) + \\ & (A^3/8) I'''(V) + \cdots] \sin(pt) - [(A^2/4) I''(V) + \\ & (A^4/48) I''''(V) + \cdots] \cos(2pt) - [(A^3/24) I'''(V) + \\ & \cdots] \sin(3pt) + [(A^4/192) I''''(V) + \cdots] \cos(4pt) \end{aligned} \tag{27}$$

If the second harmonic of the probe current is extracted by suitable filtering and amplification, the amplitude of this harmonic will be $(A^2/4) I''(V) + (A^4/48) I''''(V) + \cdots\cdots$. If the amplitude of the applied

alternating voltage, A, is made quite small, the amplitude of the second harmonic of the probe current, i, gives the form of the electron distribution function in the vicinity of the probe.

Distribution Function. Dr. G. Medicus of the Advanced Techniques Branch, Wright-Patterson Air Force Base, Ohio, in his article entitled "Theory of Electron Collection of Spherical Probes", (Ref 9:2512) develops the theory of the spherical probe in a plasma which contains a Half-Maxwellian velocity distribution of electrons. This velocity distribution is the form which is expected in a secondary plasma which is formed by accelerating electrons from a primary plasma with a positively biased gird. This is the method which was used in this study to produce the plasma in the microwave cavity. The accelerated Half-Maxwellian distribution function, normalized such that the integral over all α equals one, is given by

$$f(\alpha)=\frac{4}{\sqrt{\pi}}\alpha^2\left(1-\frac{\alpha_0}{\alpha}\right)\exp\left[-\left(\alpha^2-\alpha_0^2\right)\right] \qquad (28)$$

for $\alpha \geq \alpha_0$ and

$$f(\alpha)=0 \qquad (29)$$

for $\alpha < \alpha_0$. In this equation α is the ratio of the electron velocity to the characteristic velocity, $\sqrt{\frac{2kT}{m}}$, and α_0 is the ratio of the velocity that is imparted to an electron by the accelerating potential to the characteristic velocity.

Integral Evaluation

A computer program was written to evaluate the right side of equation (1) with the accelerated Half-Maxwellian distribution function

inserted into the integrals. The experiment was designed so that the collision frequency was much less than the microwave frequency which was used for the measurements, and the collision frequency was expressed by the equation (Ref 2:3)

$$\nu_c = P_o P_c V \tag{30}$$

where P_o is the corrected pressure in millimeters of mercury, P_c is the probability of collision (macroscopic cross section in cm^{-1} at 1 mm Hg. and 273° Kelvin), and V is the electron velocity. When the electron velocity was expressed in normalized units of α, equation (1) becomes

$$\frac{\sigma_r}{\sigma_i} = -\frac{100 P_o t}{\omega} \frac{\int_{\alpha_o}^{\infty} P_c \alpha^4 e^{-(\alpha^2-\alpha_o^2)}(2\alpha^3 - 2\alpha_o\alpha^2 - 2\alpha + \alpha_o)\,d\alpha}{\int_{\alpha_o}^{\infty} \alpha^3 e^{-(\alpha^2-\alpha_o^2)}(2\alpha^3 - 2\alpha_o\alpha^2 - 2\alpha + \alpha_o)\,d\alpha} \tag{31}$$

The constant factor in front of the integrals was evaluated using: $P_o = 1.67 \times 10^{-3}$ mm Hg. which is the corrected vapor pressure of mercury at 20°C; $t = 7.786 \times 10^5$ meters per second, the characteristic velocity of the plasma electrons; and $\omega = 1.6881 \times 10^{10}$ radians per second, the resonance frequency of the microwave cavity. The factor of 100 in the numerator is a conversion factor for changing P_c from cgs. to mks. units. This gave the equation

$$\frac{\sigma_r}{\sigma_i} = 7.735 \times 10^{-6} \frac{\int_{\alpha_o}^{\infty} P_c \alpha^4 e^{-(\alpha^2-\alpha_o^2)}(2\alpha^3 - 2\alpha_o\alpha^2 - 2\alpha + \alpha_o)\,d\alpha}{\int_{\alpha_o}^{\infty} \alpha^3 e^{-(\alpha^2-\alpha_o^2)}(2\alpha^3 - 2\alpha_o\alpha^2 - 2\alpha + \alpha_o)\,d\alpha} \tag{32}$$

Mercury. The IBM 1620 computer was used to evaluate the above

equation with values of P_c which were taken from Robert B. Brode's article, "The Quantitative Study of the Collisions of Electrons with Atoms" (Ref 1:257) (See Appendix B). The results which were obtained are tabulated in Table I below. Table I shows that the accelerating

Table I

Computed Values of the Ratio
of the Integrals in Equation (32)

Accelerating Voltage	Ratio of Integrals
1.46	1813
1.83	1791
2.28	1761
2.79	1721
3.34	1670
3.95	1604
4.60	1537
5.31	1491
6.07	1464

potential which was applied to the electrons should not have a great effect on the ratio of the integrals in equation (32) and hence on the conductivity ratio of the cavity. This is to be expected since equation (32) shows that if P_c is proportional to $1/\alpha$, the ratio of the integrals and hence the conductivity ratio becomes a constant for any type of distribution function. The probability of collision for mercury vapor is very close to a $1/\alpha$ type of function, and therefore the type of distribution function does not affect the conductivity ratio to a great extent.

An attempt was made to use a least-squares polynomial curve fitting

program that was available for the IBM 1620 computer to express the probability of collision, P_c, of mercury as a series of terms such as

$$P_c = A_1\alpha^{-3} + A_2\alpha^{-2} + A_3\alpha^{-1} + A_4 + A_5\alpha + \cdots \qquad (33)$$

If such an expression were available, then the integrals in equation (32) could be evaluated using moments of the distribution function, and the probability of collision for any type of plasma could be expressed as a series of the above type and used to evaluate the conductivity ratio. We were unable to produce a series of the above type which would give the values of P_c to the desired accuracy, but further attempts using a series of α^2 or α^3 terms might give the desired results.

Rare Gases. A computer program was written to give the ratio of the integrals in equation (32) if P_c is a constant or P_c is proportional to α. The results of the calculations are given in Table II below.

Table II

Computed Values of the Ratio of the Integrals in Equation (32) With Constant P_c and P_c Proportional to Velocity

Accelerating Voltage	Integral Ratio	
	P_c = Constant	$P_c \approx \alpha$
1.46	7.351	53.91
1.83	8.324	69.23
2.28	9.374	87.83
2.79	10.406	108.25
3.34	11.427	130.57
3.95	12.443	154.81
4.60	13.454	181.00
5.31	14.463	209.16

From Table II it can be seen that when the probability of collision is a constant or is proportional to the velocity, a change in the distribution function has a considerable effect on the conductivity ratio of the microwave cavity. Probabilities of collision of the above types are found in plasmas of the rare gases.

III. Equipment Design

The design of the microwave cavity was based on the fulfillment of two conditions which are necessary for the calculation of the conductivity ratio. First, the collision frequency of the electrons must be much less than the microwave frequency which is used for the measurements, and secondly, the mean free path of the electrons in the plasma must be long enough that the accelerated Half-Maxwellian distribution function is retained throughout the cavity and short enough that the electrons will not beam through the center of the cavity without filling it.

Mercury vapor at room temperature seemed to fulfill these criteria quite well. The collision frequency was calculated to be approximately 4×10^7 collisions per second throughout the energy range of the electrons which we would use, and the mean free path of the electrons would be approximately 2 centimeters.

Cavity Design

The dimensions of the cavity were determined from the equation

$$\lambda_R = 2.61 \times R \tag{34}$$

for the resonance wavelength, λ_R, of a cylindrical cavity of radius, R, which is resonating in the TM_{010} mode. Since the microwave equipment which was available would operate from 2 kmc (kilomegacycles) to 7.5 kmc, and the largest which could be used was desired, we decided to design for a frequency of 2.6 kmc. This fulfilled the first criteria

since the cavity frequency would be 1.63×10^{10} radians per second which is much greater than the collision frequency of 4×10^{7} collisions per second, and it allowed a margin for error since we could operate down to 2 kmc if the resonance frequency of the cavity turned out to be below the 2.6 kmc of the design.

The TM_{010} mode was used since it could be excited in the cavity by using a wire loop in the vertical plane. Since the height of a cylindrical cavity which is resonating in the TM_{010} mode is not a parameter which affects the frequency, a height of 5.5 cm was chosen for the cavity. This height was greater than two mean free paths and should allow the electrons which were drawn through the accelerating grid to diffuse throughout the cavity. A radius of 4.25 cm was calculated for the cavity from equation (34). Fig. 3 below shows a cutaway side view of the final design of the cavity. This design resulted from consultation with Dr. G. Medicus, Physicist; Mr. W. Eppers, Supervisory Physicist; and Mr. F. Ruff, Mechanical Engineer of the Advanced Techniques Branch of the Electron Technology Laboratory at Wright-Patterson Air Force Base, Ohio.

The cavity was built in five major sections (See Appendix E) that were bolted together with Viton "O" rings forming the vacuum seal between each section. This allowed us to disassemble the cavity when desired and provided for the substitution of a center section of smaller radius if a higher frequency were desired. Mild carbon steel was used for the construction except for a kovar cylinder at the bottom of the cavity which was used to facilitate the glass to metal seal at this

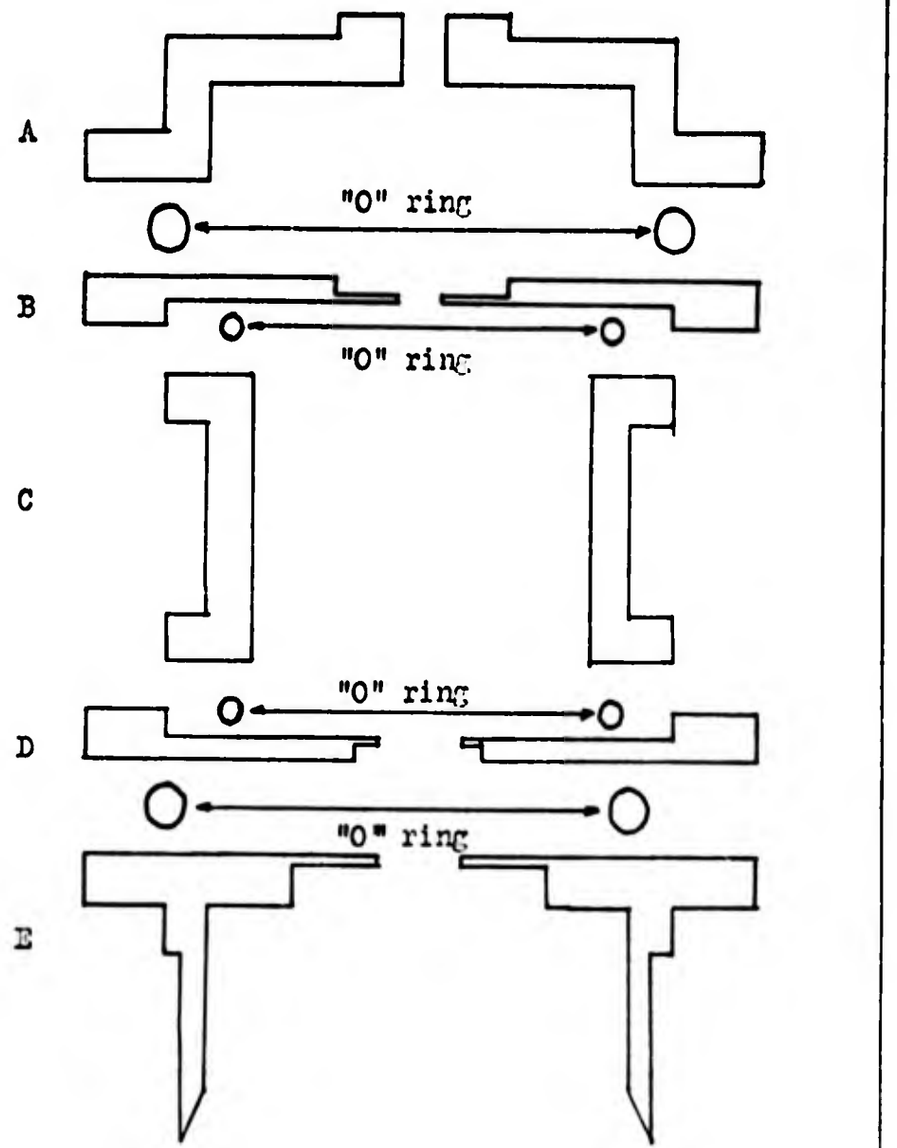

Fig. 3

Assembly Diagram of Cavity

point. The kovar cylinder was welded to the steel housing in a hydrogen induction furnace with silver solder. Sections B, C, and D of Fig. 3 were bolted together to form an electrical as well as a vacuum seal. Sections A and E (Fig. 3) were electrically insulated from the central section (B, C, and D) by using a thick "O" ring which prevented metal to metal contact between the sections and insulating inserts around the bolts which held the sections together. This allowed section E to be used as the primary anode for the plasma discharge. The central section was then biased at a positive potential with respect to the primary anode in order to accelerate the electrons into the microwave cavity which was formed by the central section. This accelerating potential imparts the initial normalized velocity, α_o, in the accelerated Half-Maxwellian distribution function which was discussed in the section on probe theory in Chapter II. Section A (Fig. 3) was biased positive with respect to the central section to extract the electrons from the cavity and prevent a space charge from forming in the cavity.

Section E, which was used as the primary anode, had a circular opening 20 mm in diameter in the center to allow the electrons to be accelerated from the primary plasma in the lower section of the tube into the microwave cavity. Section D contained a removable 0.5 mm mesh grid which was also 20 mm in diameter. When this grid was biased positively with respect to the primary anode, electrons were drawn from the primary plasma into the cavity. A 5 mm hole in the center of section B served the dual purpose of extracting electrons from the

secondary plasma in the cavity and allowing the vertical probe to be inserted into the cavity.

The glass base of the plasma tube contained the heated cathode and the vacuum line to a mercury diffusion pump. Fig. 4 is a side view of the cavity and vacuum apparatus. Appendix E contains photographs of the completed apparatus and the microwave equipment which was used in this experiment.

Microwave Circuitry

A block diagram of the microwave circuitry which was used is included as Appendix A. A Universal Klystron Power Supply (type 801A, serial no. 452, built by the Polytechnic Research and Development Co., Inc.) was used as a microwave source. The signal from the microwave supply was fed through an isolator and a directional coupler into the excitation loop of the cavity. The signal from the branch of the directional coupler was channeled into a tee. From one branch of the tee, the signal passed into a Hewlett Packard transfer oscillator (model 540A, serial no. 248) and then into a frequency counter (Hewlett Packard, model FR-38 D/U, serial no. N383-46506A). From the other branch of the tee the signal traveled into a crystal detector (Hewlett Packard, model 440A) which produced a voltage that was proportional to the microwave power into the detector. The voltage from the crystal detector was then directed into one channel of a dual channel oscilloscope.

The signal from the output loop of the cavity traveled through a Polytechnic Research and Development Company attenuator (model 175B, serial no. 330) and into a crystal detector similar to the one mentioned

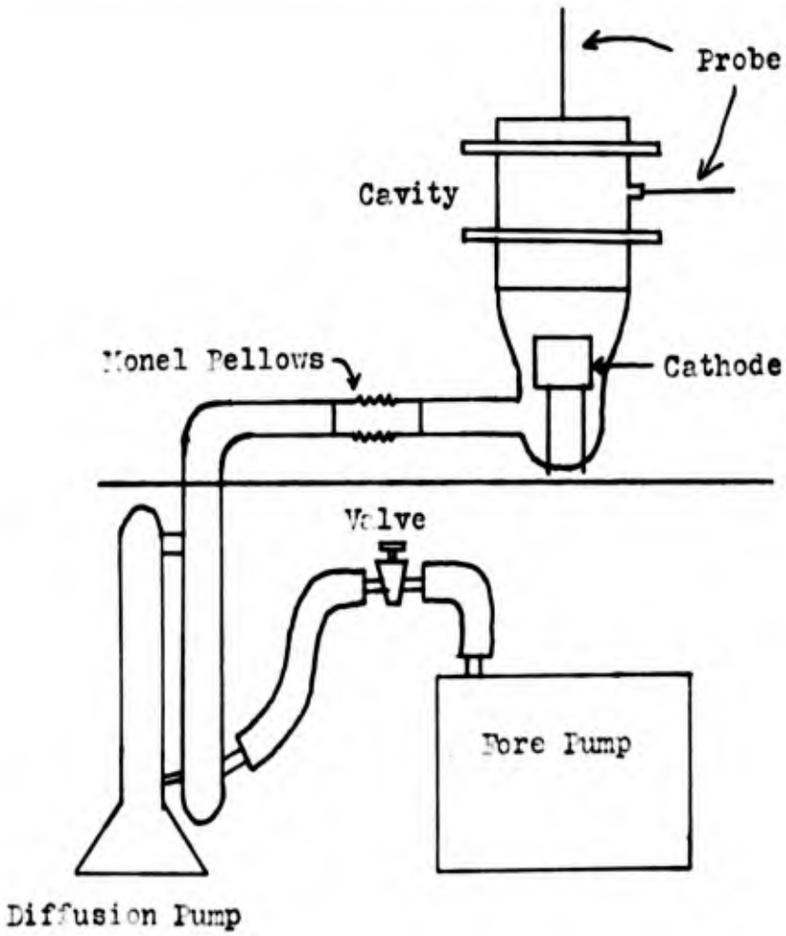

Fig. 4

Vacuum Apparatus

above. From this detector the direct current signal passed into the other channel of the oscilloscope.

With this circuitry the voltage on one channel of the oscilloscope was proportional to the microwave power which was incident into the cavity and the voltage on the other channel was proportional to the microwave power which passed through the cavity.

Probe Design

Two spherical Langmuir probes (See Fig. 5) were constructed from

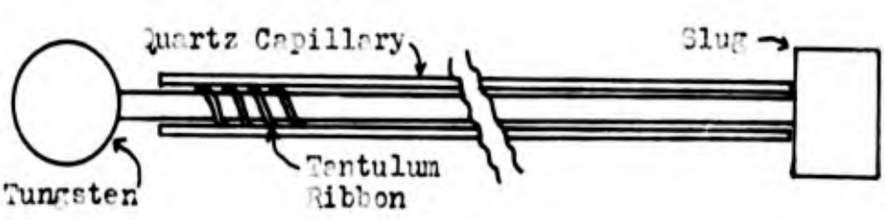

Fig. 5

Spherical Probe

0.15 mm tungsten wire for insertion into the cavity from the top and from the side. The spheres on the end of the probes were made by touching the tungsten wire against a carbon block and passing a direct current through the wire until the tip was hot. Then the wire was removed from the carbon block and an arc was formed. This process formed a sphere on the end of the wire. The vertical probe which was used in

this experiment was 0.60 mm in diameter and the horizontal probe was 0.61 mm in diameter.

After the tungsten probes were formed, the wire was wrapped with a tantulum ribbon which served as a spacer and inserted into a quartz capillary tube. The tantulum spacer separated the end of the quartz capillary from the tungsten wire. This separation was necessary since metallic vapor which collects on the end of the quartz capillary would make electrical contact with the probe wire if spacing were not provided. The final step in the preparation of the probe was the soldering of the end of the tungsten wire to a ferrous slug. This slug was cylindrical with a diameter such that it slides inside a cylindrical monel tube (See Fig. 6).

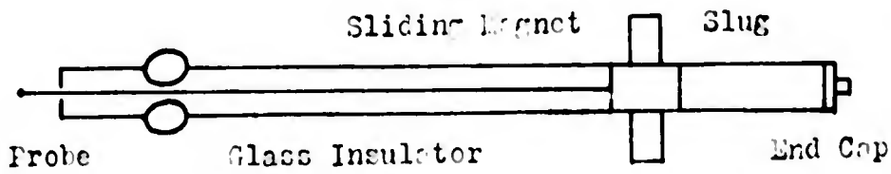

Fig. 6

Probe Holder

The probe is held by friction in the probe holder tube (Fig. 6). A magnet, which can be moved along the length of the probe holder, controls the extension and retraction of the probe. Electrical contact

with the probe is made through the slug to the probe holder. This arrangement allowed the vertical probe to be moved from the top to the bottom of the cavity along the central axis. The horizontal probe was of similar construction, but it was attached to the side of the cavity by a molybdenum bellows which allowed it to be pivoted vertically and horizontally as well as extending and retracting. This probe arrangement allowed us to take probe measurements at any position in one-half of the cavity on the side opposite to the horizontal probe. Since the plasma in the cavity is radially symethrical, this was sufficient for the experiment.

IV. Experimental Procedure

Microwave Measurements

Trial Measurements. The microwave measurements were made by first adjusting the klystron supply to sweep through a frequency band and then adjusting the frequency band until the resonance frequency of the cavity was found. This resonance condition appeared as a peak in the transmitted power channel of the oscilloscope. The klystron supply was then switched to a fixed frequency output, and the frequency was adjusted until the power in the transmitted channel was a maximum. This frequency was the resonance frequency of the cavity. The variable attenuator in the transmitted power channel was then set to 8.06 db. This setting was selected since a larger attenuation reduced the transmitted signal below a readable level and a smaller attenuation did not provide for sufficient attenuation decrease to perform the experiment. The traces from the two channels on the oscilloscope were then adjusted by using the gain controls of the oscilloscope until they were superimposed. This gave the null condition which was desired. The attenuation in the transmitted power channel was then decreased resulting in a voltage increase in the transmitted power channel and a rise in the trace corresponding to this channel on the oscilloscope. The power in the transmitted channel was then decreased back to the null position by adjusting the frequency until it was slightly greater or less than the cavity resonance frequency. When the apparatus was in the null position, the transfer oscillator was tuned to give a beat frequency

with the klystron frequency, and the transfer oscillator frequency was measured with the frequency counter. Since the seventeenth harmonic was used, the klystron frequency was then calculated to be seventeen times the frequency of the transfer oscillator. The frequency below the resonance frequency, which gave a null condition after the variable attenuator was decreased, was called ω_1, and the corresponding frequency above the resonance frequency was called ω_2. The quantity X in equation (13) was then set equal to $\omega_2 - \omega_1$. This involved the assumption that the resonance curve of power transmitted through the cavity vs frequency was symmetrical above the resonance frequency. This assumption limited the amount of attenuation which could be used in the experiment since it was found that the resonance curve was not symmetrical at frequencies which differ from the resonance frequency by more than 1 mc. The attenuation change was therefore limited to a 4 db decrease. If larger attenuation decreases were attempted, the plot of A, the power ratio, against X^2 did not give a straight line but began to be concaved upward for the higher values of X^2 (See Fig. 6a).

Final Measurements. Three attenuator settings were chosen for the final experimental measurements. These corresponded to an attenuation of 6.57 db, 5.16 db, and 4.05 db. The null frequencies, ω_1 and ω_2 were measured at each of these attenuator settings and the plot of A vs X^2 was constructed from these data. The null frequencies were measured seven times during each run in order to obtain statistical reliability. Five different plasma conditions were analysed in this

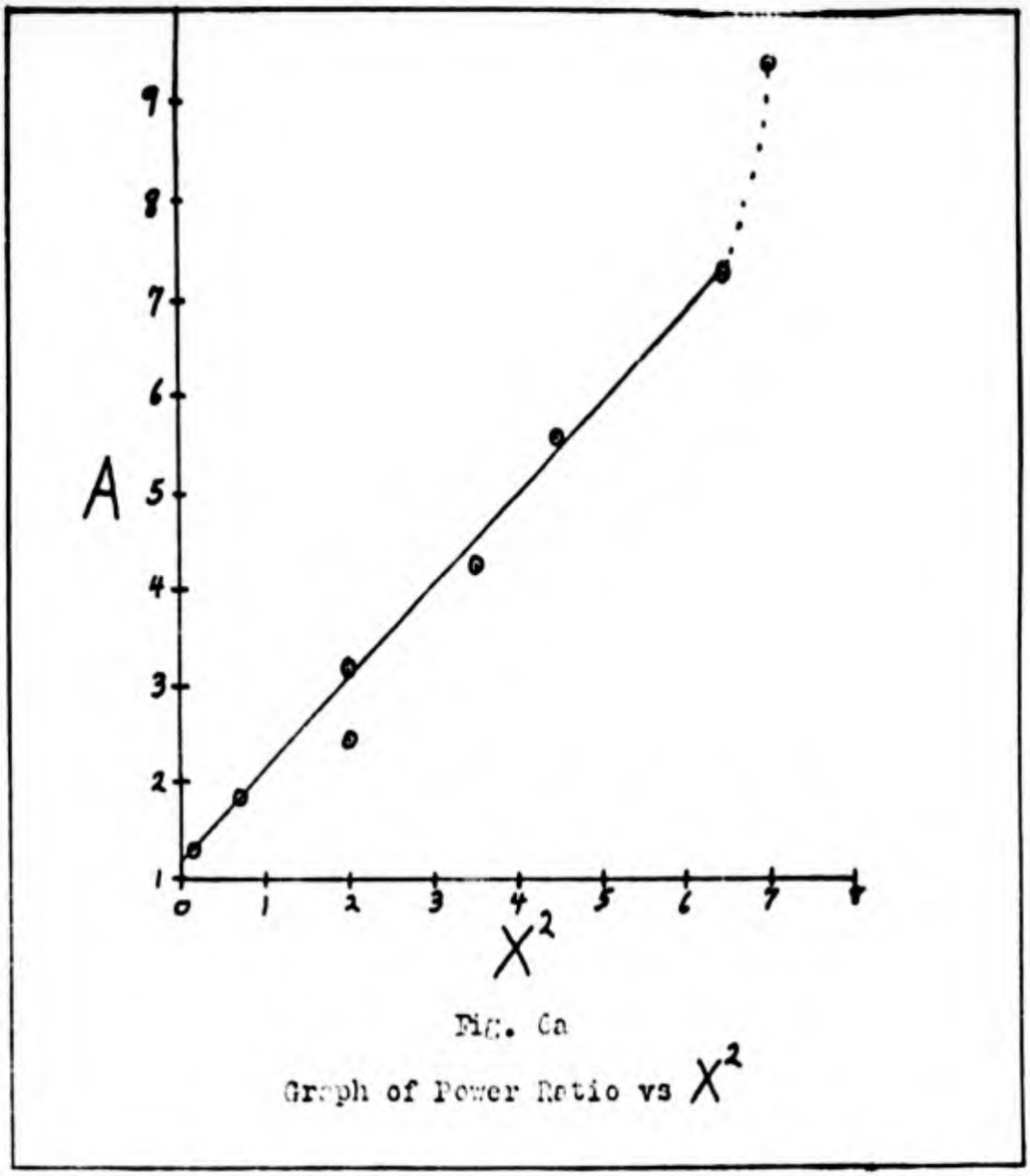

Fig. 6a

Graph of Power Ratio vs X^2

manner.

First, the experiment was carried out without a plasma in the cavity to obtain the initial data which was necessary for the calculations. Then the plasma tube was ignited, and a series of measurements were taken with no potential difference between the cavity and the anode $(V_0 = 0)$. This indicated if any plasma was streaming through the grid into the cavity without the application of an accelerating

potential to the cavity. After these runs were completed a series of measurements were made with the cavity biased positive with respect to the anode at values of 2.28 volts, 3.95 volts, and 5.30 volts.

Probe Measurements

After the microwave measurements were completed a spherical Langmuir probe was inserted into the cavity from the top and from the side in order to obtain probe curves and second derivative curves of the plasma. The plasma was adjusted until the conditions of the plasma were the same as those which were used for the microwave measurements at an accelerating voltage of 3.95 volts.

V. Data Processing and Results

Data Processing

The slope of the plot of A vs X^2 was calculated from the data obtained by the method described in the previous chapter. In order to expedite the calculation of this slope, and to avoid the errors which would be introduced by plotting a series of points and attempting to draw a straight line through them, the best least-squares fit of a straight line to the data points was used. P. G. Hoel's Introduction To Mathematical Statistics (Ref 5:79, 80) was consulted and a computer program (see Appendix C) was written to process the data. This computer program gave the slope Z (corresponding to BR/C in equation (24)); the intercept, BB (corresponding to R/C in equation (24)); the corrected slope, ZC, (corresponding to B in equation (23)); the square root of the reciprocal of the corrected slope, AA (corresponding to α in equation (25)); the square of the standard deviation, $ESAA$, in AA; and the resonance frequency of the cavity, WO (corresponding to ω_0 in equation (12)), with the square of the standard deviation, $ESWO$, in WO.

This computer program required input data which consisted of a lead card containing the number of points in the run and the original attenuator setting and a series of data cards containing the null frequencies, ω_1 and ω_2, and the attenuator settings at which the null was obtained. The computer calculated and printed the values of A and X^2 for each point and the information referred to in the para-

graph above. The computer output also indicated the deviation of each data point from the best least-squares line. The computer output gave all of the information which was necessary to compute the conductivity ratio of the plasma. It was also possible, by using the deviations of the data points from the least-squares line, to remove any data points which appeared to have been in error.

The conductivity ratio was then calculated from the equation

$$\frac{\sigma_n}{\sigma_i} = \frac{\Delta\alpha}{2(\omega_0 - \omega_0')} \tag{35}$$

which is a combination of equations (17) and (18).

Results

The conductivity ratios which were obtained from the microwave measurements and those which were calculated from equation (32) are given in tabular form in Table III below.

Table III

Experimental and Theoretical Values of the Plasma Conductivity Ratio

Accelerating Potential (Volts)	α			α	ω_o	σ_n/σ_i	σ_n/σ_i
	21 Data Points	19 Data Points	17 Data Points	(Best Value)		(Microwave Measurement)	(Theoretical Calculation)
No Plasma	$1.34 \pm \sqrt{0.0111}$	$1.35 \pm \sqrt{0.0076}$	$1.32 \pm \sqrt{0.0045}$	$1.33 \pm \sqrt{0.0045}$	$2688.42 \pm \sqrt{0.0002}$		
0.00	$1.40 \pm \sqrt{0.0196}$	$1.40 \pm \sqrt{0.0095}$	$1.32 \pm \sqrt{0.0052}$	$1.40 \pm \sqrt{0.0095}$	$2693.12 \pm \sqrt{0.02}$	$0.00745 \pm \sqrt{0.01260}$	
2.28	$1.43 \pm \sqrt{0.0118}$	$1.48 \pm \sqrt{0.0082}$	$1.50 \pm \sqrt{0.0079}$	$1.48 \pm \sqrt{0.0082}$	$2692.24 \pm \sqrt{0.01}$	$0.0197 \pm \sqrt{0.01480}$	0.01362
3.95	$1.34 \pm \sqrt{0.0040}$	$1.40 \pm \sqrt{0.0026}$	$1.44 \pm \sqrt{0.0013}$	$1.44 \pm \sqrt{0.013}$	$2691.13 \pm \sqrt{0.003}$	$0.0203 \pm \sqrt{0.01400}$	0.01241
5.30	$1.60 \pm \sqrt{0.0138}$	$1.65 \pm \sqrt{0.0107}$	$1.74 \pm \sqrt{0.0083}$	$1.70 \pm \sqrt{0.0083}$	$2691.17 \pm \sqrt{0.02}$	$0.0674 \pm \sqrt{0.00802}$	0.01154

VI. Discussion and Recommendations

Discussion

Microwave Measurements. When the previously discussed experimental procedure was attempted, several problems manifested themselves. When the microwave procedure was used without a plasma in the cavity, the background noise in the microwave circuit made the measurements difficult and inaccurate. The trace on the oscilloscope from the input power channel was approximately 0.5 cm wide while the trace on the transmitted power channel was 0.75 cm wide. The latter showed a wider trace from noise since this circuit required an amplifier which amplified the signal 500 times. The amplifier was necessary because of the low level in the microwave power which was transmitted through the cavity. The transmitted power channel also picked up a sixty cycle waveform from the circuit leads and the amplifier. Fig. 7 shows the approximate waveforms which were observed on the oscilloscope when the traces were not in the nulled position. It can be seen that an accurate adjustment of the null position was extremely difficult.

The null was adjusted at the beginning of each data run, with the attenuator set at 8.06 db, and twenty-one readings were taken at that particular plasma condition. This required approximately twenty minutes. After each run the attenuator was returned to a setting of 8.06 db and the null condition was rechecked. This check indicated that in most cases the equipment was drifting from the null position due to a variation in the relative gains of the two circuits during the period in

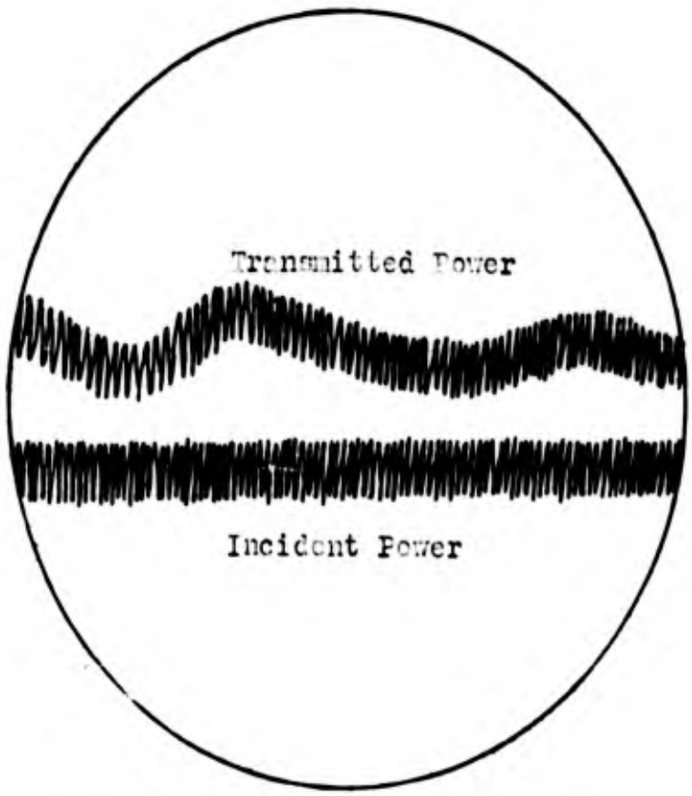

Fig. 7

Oscilloscope Traces at Resonance Frequency

which the data was recorded. This variation resulted in a dispersion of the points on the plot of A vs X^2 and a large standard deviation in α. This is confirmed by the data in Table III since the measurement with V_0 = 3.95 volts was the only run in which the equipment did not drift out of a null condition. The standard deviation of this run is only one-half the standard deviations of the measurements in which

the equipment drifted out of a null condition.

The equipment cannot be reset to the null condition during the data run because the adjustment of the null causes some error in the slope of the plot of γ vs X^2. In Chapter II, the correction which was used to compensate for an incorrectly adjusted null position was discussed. This compensating correction can only be applied when the null setting remains a constant. Better shielding of the circuit leads and better grounding of the equipment could reduce the sixty-cycle waveform on the oscilloscope, but experimental apparatus of better design would be necessary to reduce the background noise and drifting gains of the circuits.

When the plasma discharge in the tube was ignited in order to introduce a secondary plasma into the cavity, it was apparent that a secondary plasma was being formed without an accelerating potential to draw the electrons upward into the cavity. Some electrons were streaming through the hole in the anode and through the accelerating grid even though there was no potential applied. The cavity became approximately 7 volts negative with respect to the anode from the electron space charge which was introduced into the cavity by the streaming electrons. When the plasma tube was operated with an anode current of 2 amperes the microwave characteristics of the cavity changed drastically from those of the empty cavity. The resonance frequency increased and the cavity resonance curve became skewed (see Fig. 8). This indicated that the basic assumption that the plasma does not effect the electric field of the cavity was not valid. In order to

return the cavity resonance curve to its normal symmetrical shape, the anode current of the plasma tube was reduced. This reduction in anode current reduced the resonance frequency of the cavity and decreased the skewing of the resonance curve, but a limiting point

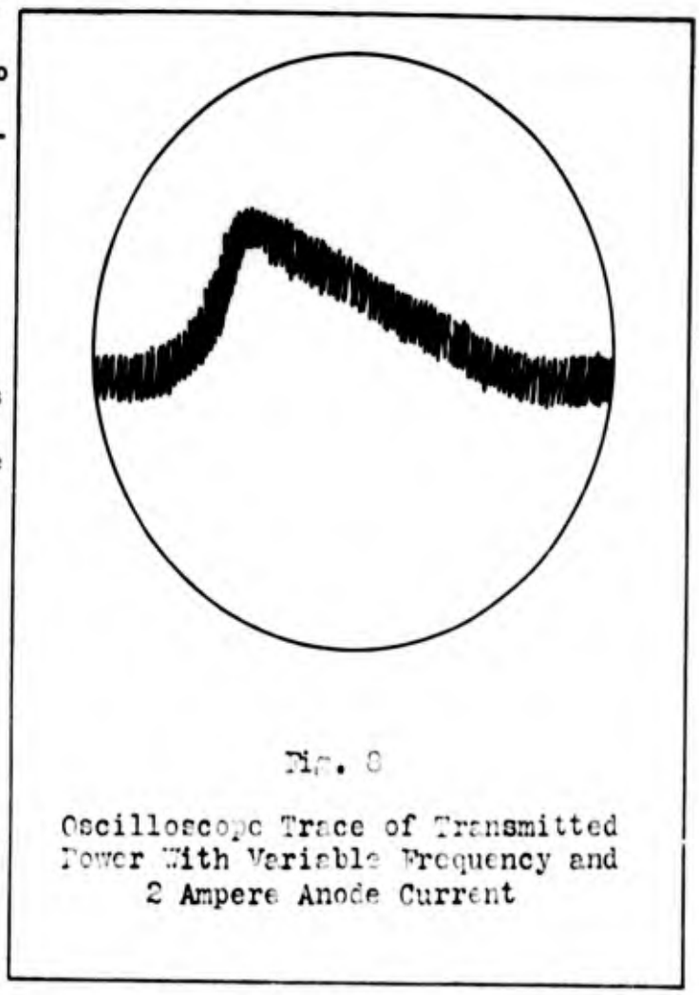

Fig. 8

Oscilloscope Trace of Transmitted Power With Variable Frequency and 2 Ampere Anode Current

was reached at which the plasma tube went out. The four data runs which are listed in Table III were carried out with an anode current of 120 ma in the plasma tube. This gave an oscilloscope trace similar to Fig. 9. The skewing of the cavity resonance curve and the increase of the resonance frequency indicated that the plasma density in the cavity must be maintained at a very low level. This could be accomplished by several methods.

Fig. 10 indicates an arrangement of the anode and cathode which should be more satisfactory in reducing the plasma density in the

cavity. A smaller cathode would also be desirable in this arrangement since the cathode which was used (from a 4C35) was quite large, and when it was operated at 120 ma, only parts of it emitted electrons. The emitting sections of the cathode varied with time and the anode current was unsteady. This introduced additional errors into the experiment.

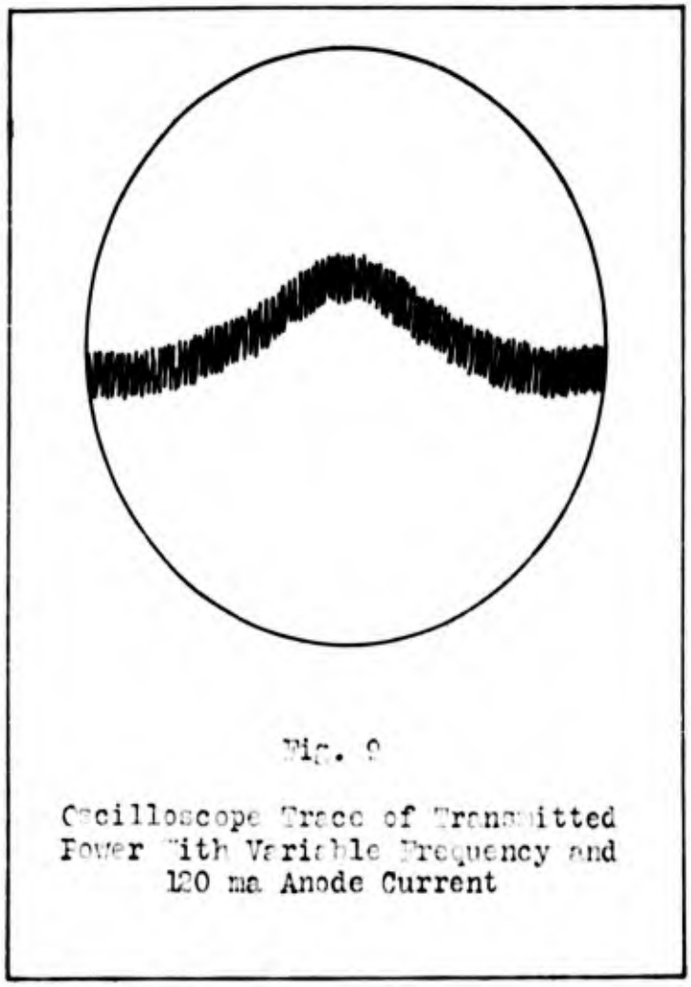

Fig. 9

Oscilloscope Trace of Transmitted Power With Variable Frequency and 120 ma Anode Current

The anode of the present configuration could be improved by having a grid installed in the hole in the center of the top plate. This grid should reduce the number of electrons which stream into the cavity. If this double grid arrangement was installed (see Fig. 11), a variable iris diaphragm could be used between the grids to reduce the plasma density in the cavity. With this arrangement the plasma density in

the cavity could be reduced to the desired value without the primary plasma going out.

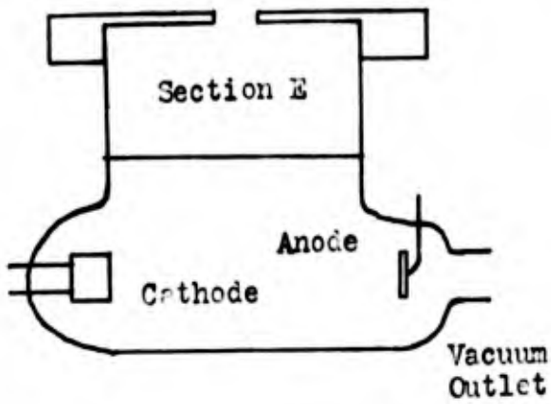

Fig. 10

Recommended Anode and Cathode Arrangement

Probe Measurements. Probe curves of the plasma were taken in the cavity using the vertical and horizontal probes. The results of these measurements were inconclusive since the noise level of the plasma combined with the high noise level of the second derivative apparatus to make it impossible to interpret second derivative curves of the plasma. The curves of the probe current vs probe voltage indicated the

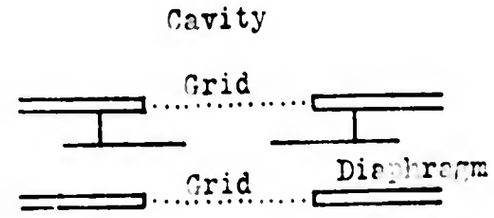

Fig. 11

Double Grid and Diaphragm Arrangement

usual fast and slow groups of electrons and a decrease in the plasma density in the cavity as the distance from the accelerating grid increases. Since the second derivative curves were unreadable the distribution function of the electrons in the plasma could not be found. The horizontal probe indicated that the secondary plasma was beaming through the grid. Measurements as far as 2 cm from the cavity walls indicated that an insignificant amount of plasma existed in this region. This was the result of the fast group electrons with their long mean free path beaming through the grid. The tube design which is depicted in Fig. 10 with a double grid arrangement such as that indicated in Fig. 11 could remedy this by placing the first grid at the same potential as the cathode. This would stop the fast group of electrons and allow a true accelerated Half-Maxwellian distribution to be drawn into the cavity. The grid used in this tube design should be of approximately 0.1 mm mesh or smaller since this is the Debye length of the electrons in the cavity. The grid which was used in this experiment had a 0.5 mm mesh which allowed the fast group electrons to beam through.

Results. Table III shows that the conductivity ratio which was obtained from the microwave measurements with an accelerating potential of 2.28 volts agreed with the calculated values from microwave theory to within 45% while the standard deviation in the microwave measurement was 75%. The results for an accelerating potential of 3.95 volts show an agreement to within 64% while the standard deviation in the microwave measurement was 70%. This indicates that the null method can be used successfully to find the conductivity ratio of the plasma

in the microwave cavity if suitable modifications are made on the equipment to improve the accuracy of the measurements. A comparison of the theoretical and experimental conductivity ratios for V_0 = 5.30 volts indicates that the procedure is not valid if the mercury plasma ionizes. The measurements must be limited to accelerating potentials below the first resonance potential of mercury which occurs at 4.88 volts. This limited range combined with the $1/\alpha$ type probability of collision for mercury makes it difficult to verify the electron distribution function which exists in the plasma.

Recommendations

Further studies using this correlation method should be attempted with plasmas of the noble gases. Neon should be an excellent choice since the probability of collision of neon is almost a constant and the first ionization potential occurs at 16 volts.

Two approaches could be used in future correlation studies. The electron velocity distribution could be measured using a spherical Langmuir probe and the second derivative technique, and the distribution function which was obtained could be inserted into equation (1) to obtain the correlation. This was the method which was used in the present study, but the second derivative apparatus was not available to give a velocity distribution from a spherical probe.

Another approach which could be used would be to obtain the df in equation (1) directly, point by point, from probe measurements. It can be shown (see Appendix D) that

$$f\left(\sqrt{\frac{2eV}{m}}\right) = \frac{\sqrt{32}\,(mV)^{3/2}}{e^{3/2}F}\left(\frac{d^3i}{dV^3} + \frac{1}{V}\frac{d^2i}{dV^2}\right) \qquad (36)$$

where V is the probe voltage, i is the probe current, and F is the effective electrode area of the probe. The electron apparatus which measures the second derivative of the probe current with respect to the probe voltage could be modified so that it will also give the third derivative. The quantity dF could then be computed and used in a computer to evaluate the integrals in equation (1). This should give the desired correlation with the ratio of the conductivities which is measured by the null method.

VII. Conclusions

The original problem of correlating the electron velocity distribution which is obtained with a spherical Langmuir probe has not been solved, but the method which was used indicates that further studies along these lines should give the desired results. The plasma tube design indicated in Fig. 10 and the double grid and iris diaphragm in Fig. 11 should allow the plasma density to be decreased so that acceptable measurements could be recorded. If the lower grid were biased to cathode potential the fast group of electrons would be removed and the accelerated Half-Maxwellian distribution function should predominate within the cavity.

In order to verify the electron velocity distribution in the plasma by the microwave method, the mercury plasma will have to be abandoned and the apparatus redesigned for use with a rare gas plasma. This is necessary since the $1/\alpha$ type probability of collision for mercury effectively masks the effect of the electron velocity distribution on the conductivity ratio of the plasma.

Bibliography

1. Brode, Robert B. "The Quantitative Study of the Collisions of Electrons with Atoms." Reviews of Modern Physics, 5:257 (1933).

2. Brown, Sanborn C. Basic Data of Plasma Physics. Boston: The Technology Press of the Massachusetts Institute of Technology, 1959.

3. Druyvesteyn, M. J. "Der Niedervoltbogen." Zeitschrift fur Physik, 64:790 (1930).

4. Gould L., and S. C. Brown. "Methods of Measuring the Properties of Ionized Gases at High Frequencies, IV. A Null Method of Measuring the Discharge Admittance." Journal of Applied Physics, 24:1053 (August 1953).

5. Hoel, P. G. Introduction to Mathematical Statistics. New York: John Wiley and Sons, 1954.

6. Jones, R. C., et al. Comparison of Microwave and Langmuir Probe Techniques for the Investigation of Electrical Discharges. U. S. Naval Research Laboratory Report Number 5468. Washington: GPO, 1960.

7. Loeb, L. B. Basic Processes of Gaseous Electronics. Los Angeles: University of California Press, 1955.

8. Margenau, H. "Conduction and Dispersion of Ionized Gases at High Frequencies." Physical Review, 69:508 (1946).

9. Medicus, G. "Theory of Electron Collection of Spherical Probes." Journal of Applied Physics, 32:2512 (1961).

10. Rose, D. J., and S. C. Brown. "Methods of Measuring the Properties of Ionized Gases at High Frequencies, I. Measurements of Q." Journal of Applied Physics, 23:711 (July 1952).

11. -----. "Methods of Measuring the Properties of Ionized Gases at High Frequencies, II. Measurement of Electric Field." Journal of Applied Physics, 23:719 (July 1952).

12. -----. "Methods of Measuring the Properties of Ionized Gases at High Frequencies, III. Measurement of Discharge Admittance and Electron Density." Journal of Applied Physics, 23:1028 (September 1952).

General References

Anderson, J. M. Applicability of the Langmuir Metallic Probe For Study of the Ultimate Electrons of the Negative Glow Plasma. Report Number 58-RL-2010. Schenectady, New York: General Electric Research Laboratory, 1958.

Brode, Robert B. "The Absorption Coefficient For Slow Electrons in Cadmium and Zinc Vapors." Physical Review, 35:504 (1930).

Cobine, J. D. Gaseous Conductors (Third Impression). New York: McGrew-Hill, 1941.

Federer, W. T. Experimental Design. New York: The MacMillan Co., 1955.

Golant, V. E. "Microwave Plasma Diagnostic Techniques." Soviet Physics, Technical Physics, 5:1197 (May 1961).

Loeb, L. B. Fundamental Processes of Electrical Discharge in Gases. New York: John Wiley and Sons, 1939.

Margenau, H. "Theory of High Frequency Gas Discharges, I., Methods For Calculating Electron Distribution Functions." Physical Review, 73:297 (1948).

Millman, J., and S. Seely. Electronics. New York: McGraw-Hill, 1941.

Penning, F. M. Electrical Discharges in Gases. New York: The MacMillan Co., 1957.

Schulz, G. J., and S. C. Brown. "Microwave Study of Positive Ion Collection by Probes." Physical Review, 98:1642 (1955).

Von Engel, A. Ionized Gases. Oxford: Clareadon Press, 1955.

Appendix A

Block Diagram of Microwave Circuitry

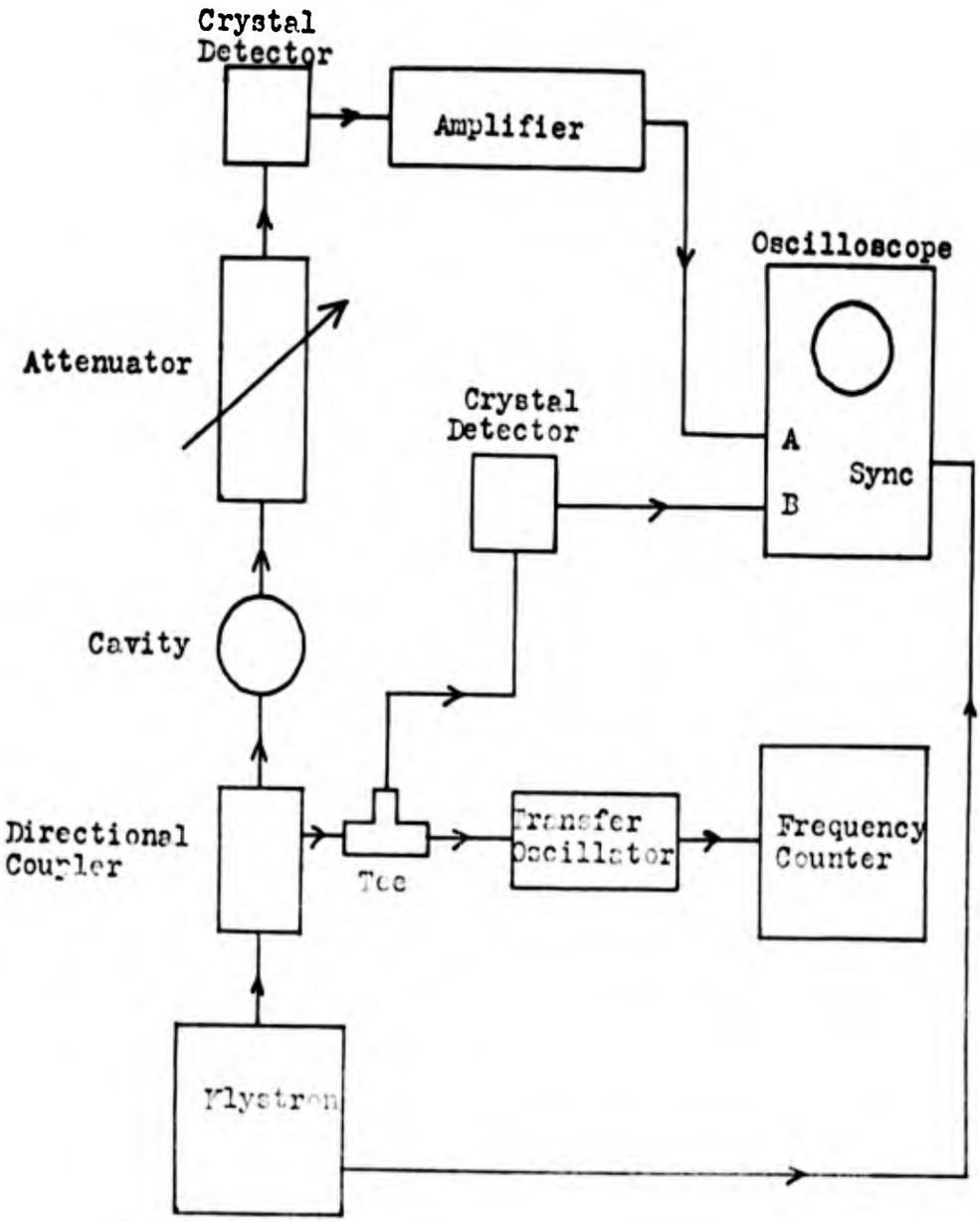

Appendix B

Computer Program to Evaluate the Integrals in Equation (1)

```
      DIMENSION A(120),P(120)
3     FORMAT (/5HAREA=E14.8)
      DO 11 I=1,120
11    READ,A(I),P(I)
18    IF (SENSE SWITCH 1) 13,14
13    DO 15 I=1,120
15    P(I)=1.
14    ACCEPT,N,J,T
      K=J+1
      A0=A(J)
      SUM=0.
      B=P(J)*A(J)**N
      C=A0/2.-A(J)
      SUM=SUM+B*C
      DO 10 I=K,119
      B=P(I)*A(I)**N*EXPF(-((A(I)*T)**2-((A0*T)**2)))
      F=EXPF((-((A(I)*T)**2-((A0*T)**2)))-1.0E-95)
      IF (F)17,17,16
16    C=2.*A(I)**3-2.*A0*A(I)**2-2.*A(I)+A0
10    SUM=SUM+B*C
17    AREA=SUM*0.1
      PRINT 3,AREA
      PAUSE
      GO TO 18
      END
```

Appendix C

Least-Squares Computer Program for Determining the Slope, of χ vs χ^2, and Sample Results

```
      DIMENSION G(60),A(60),B(60),E(60),H(60),D(60)
1     FORMAT(6X,I3,F6.3)
2     FORMAT(6X,F9.4,F9.4,F6.3)
3     FORMAT (6X,2HZ=F8.5,3X,3HBB=F8.5)
4     FORMAT(6X,4HESZ=F11.8,3X,5HESBB=F11.8)
5     FORMAT(6X,5HESRZ=F11.8,3X,6HESRBB=F11.8)
6     FORMAT(6X,3HZC=F7.4,3X,3HAA=F8.5,3X,5HESAA=F11.8)
7     FORMAT(6X,3HWO=F10.4,3X,5HESWO=F11.8)
77    FORMAT (6X,F10.4,3X,F11.6,3X,F11.6,3X,F11.8)
8     ACCN=0.
      ACCP=0.
      ACCR=0.
      ACCT=0.
      ACC=0.
      ACCU=0.
      ACCY=0.
      READ 1,N,F
      DO 9 I=1,N
      READ 2,A(I),B(I),G(I)
      E(I)=(B(I)-A(I))**2
9     H(I)=10.**((F-G(I))/10.)
      DO 10 I=1,N
      ACCN=ACCN+((B(I)-A(I))**2)*H(I)
      ACCP=ACCP+(B(I)-A(I))**2
      ACCR=ACCR+H(I)
10    ACCT=ACCT+(B(I)-A(I))**4
      ZN=N
      ZO=ACCN/ZN
      Q=ACCP/ZN
      S=ACCR/ZN
      U=ACCT/ZN
      Z=(ZO-Q*S)/(U-Q*Q)
      BB=S-Z*Q
      DD=Z*Q
      DO 11 I=1,N
      D(I)=Z*((B(I)-A(I))**2)+S-DD-H(I)
11    ACC=ACC+(D(I))**2
      ESZ=ACC/(ZN*(ZN-2.)*(U-Q*Q))
      ESBB=U*ESZ
      ZC=Z/ABS(BB)
      ESRZ=(SQRTF(ABS(ESZ))/Z)**2
      ESRBB=(SQRTF(ABS(ESBB))/BB)**2
      AA=1./SQRTF(ZC)
```

```
      ESAA=((SQRTF((ESRZ+ESRBB)/2.))*AA)**2
      DO 12 I=1,N
12    ACCU=ACCU+.5*(B(I)+A(I))
      WØ=ACCU/ZN
      DØ 13 I=1,N
13    ACCY=ACCY+(.5*(B(I)+A(I))-WØ)**2
      ESWØ=ACCY/ZN
      IF(SENSE SWITCH 1) 14,15
14    PRINT 3,Z,BB
      PRINT 4,ESZ,ESBB
      PRINT 5,ESRZ,ESRBB
      PRINT 6,ZC,AA,ESAA
      PRINT 7,WØ,ESWØ
      DØ 16 I=1,N
16    PRINT 77,A(I),H(I),E(I),D(I)
15    PUNCH 3,Z,BB
      PUNCH 4,ESZ,ESBB
      PUNCH 5,ESRZ,ESRBB
      PUNCH 6,ZC,AA,ESAA
      PUNCH 7,WØ,ESWØ
      DØ 17 I=1,N
17    PUNCH 77,A(I),H(I),E(I),D(I)
      PAUSE
      GØ TØ 8
      END
```

V_0=3.95 volts
Z= .48867 BB= .88393
ESZ= .00038203 ESBB= .00216670
ESRZ= .00159977 ESRBB= .00277307
ZC= .5528 AA= 1.34492 ESAA= .00395487
WØ= 2691.1363 ESWØ= .00261268

2690.6512	1.409288	.955506	-.05842200
2690.3656	1.949844	2.304627	.06030550
2690.1871	2.517676	3.567187	.10945620
2690.6716	1.409288	1.110916	.01752300
2690.4540	1.949844	2.253301	.03522360
2690.3248	2.517676	3.192296	-.07374390
2690.5509	1.409288	1.448653	.10256700
2690.3809	1.949844	2.097862	-.04073560
2690.0953	2.517676	3.477852	.06580000
2690.5934	1.409288	1.068329	-.00328820
2690.3826	1.949844	2.048906	-.06465950
2690.1191	2.517676	3.496900	.07510830
2690.5628	1.409288	1.096627	.01054070
2690.3503	1.949844	2.227854	.02278850
2690.2500	2.517676	3.024468	-.15575750
2690.6444	1.409288	.968046	-.05190300
2690.3945	1.949844	2.157373	-.01165410
2690.2279	2.517676	3.395911	.02575700
2690.6274	1.409288	1.147041	.03517640
2690.4744	1.949844	2.107723	-.03591690
2690.3537	2.517676	3.048166	-.14417690

Appendix D

Derivation of df

Equation (26) is used to find df by differentiating each side of the equation with respect to V. This gives

$$\frac{d^3i}{dV^3} = \frac{e^2F}{4m}\left[\sqrt{\frac{e}{2m}}\, f'\left(\sqrt{\frac{2eV}{m}}\right)\frac{1}{V^{3/2}} - \frac{1}{V^2} f\left(\sqrt{\frac{2eV}{m}}\right)\right] \tag{37}$$

If $f\left(\sqrt{\frac{2eV}{m}}\right)$ from equation (26) is substituted into equation (37), the result is

$$\frac{d^3i}{dV^3} = \frac{e^2F}{4m}\left[\sqrt{\frac{e}{2m}}\,\frac{1}{V^{3/2}} f'\left(\sqrt{\frac{2eV}{m}}\right) - \frac{4m}{e^2FV}\,\frac{d^2i}{dV^2}\right] \tag{38}$$

When equation (38) is solved for $f'\left(\sqrt{\frac{2eV}{m}}\right)$ and the substitution

$$v = \sqrt{\frac{2eV}{m}} \tag{39}$$

is made, the resulting equation is

$$df = \frac{\sqrt{32}\,(mV)^{3/2}}{e^{3/2}\,F}\left(\frac{d^3i}{dV^3} + \frac{1}{V}\,\frac{d^2i}{dV^2}\right) \tag{40}$$

Appendix E

Drawings and Photographs of Microwave Cavity

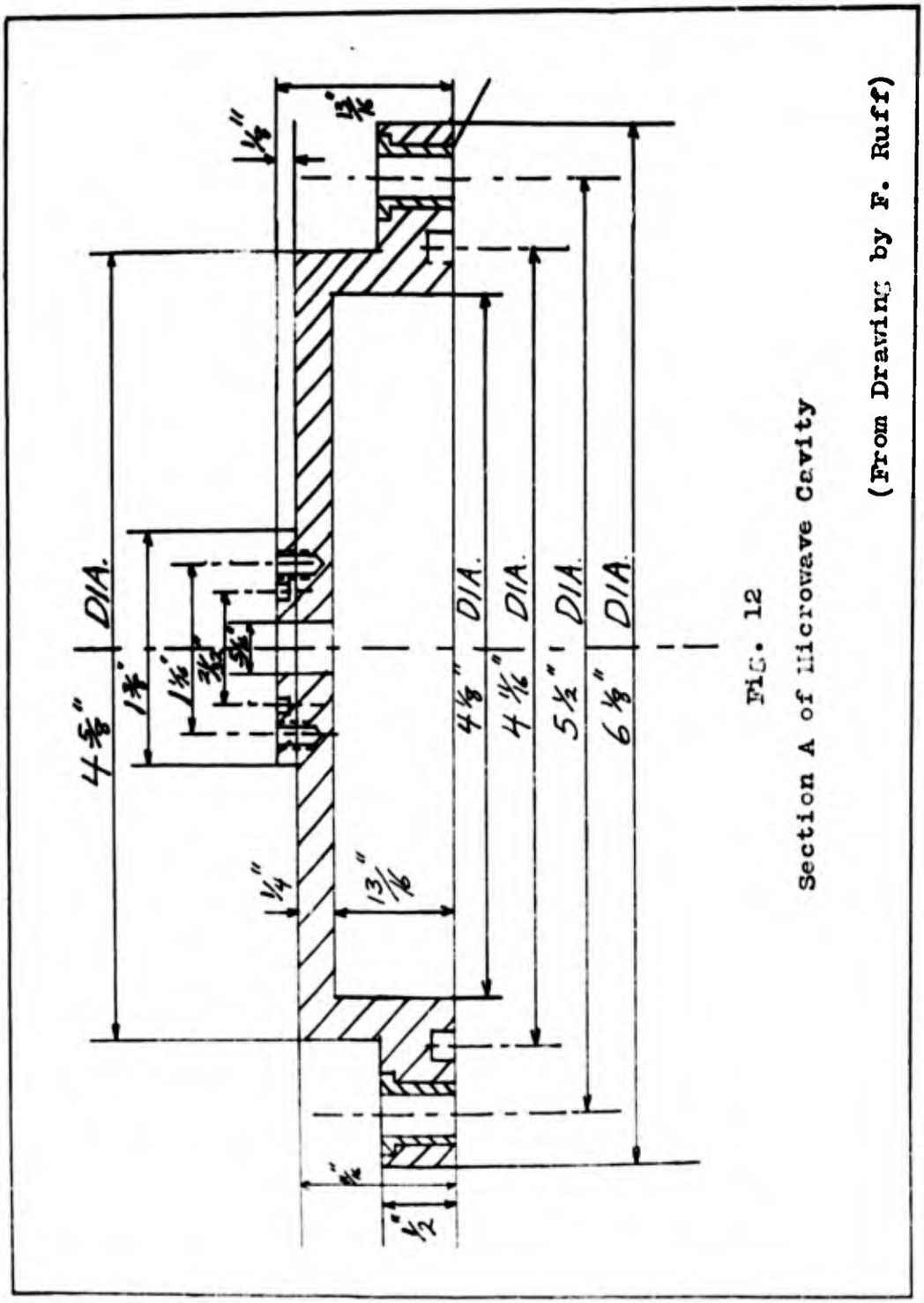

Section A of Microwave Cavity (From Drawing by F. Ruff)

Fig. 12

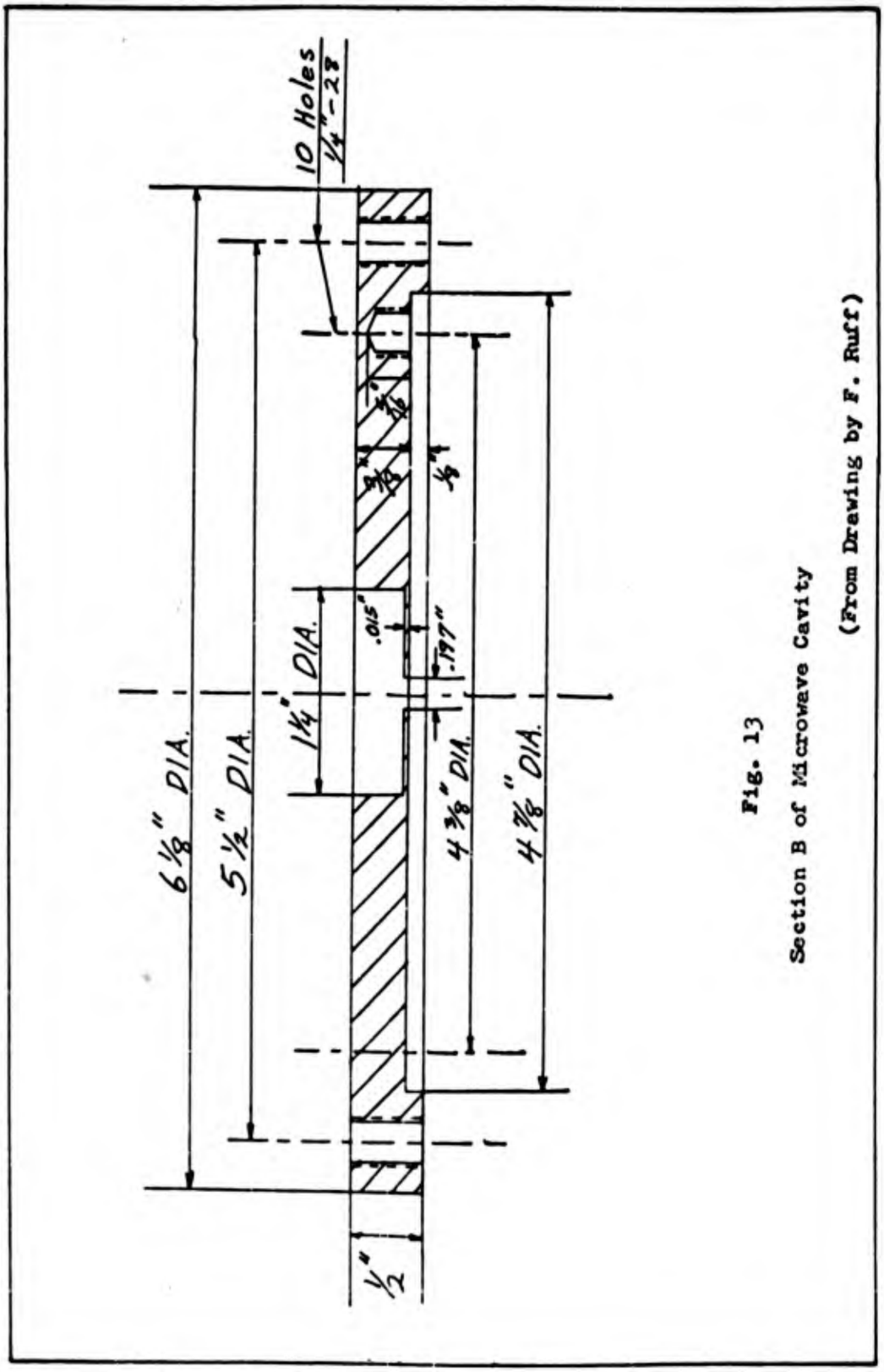

Fig. 13

Section B of Microwave Cavity

(From Drawing by F. Ruff)

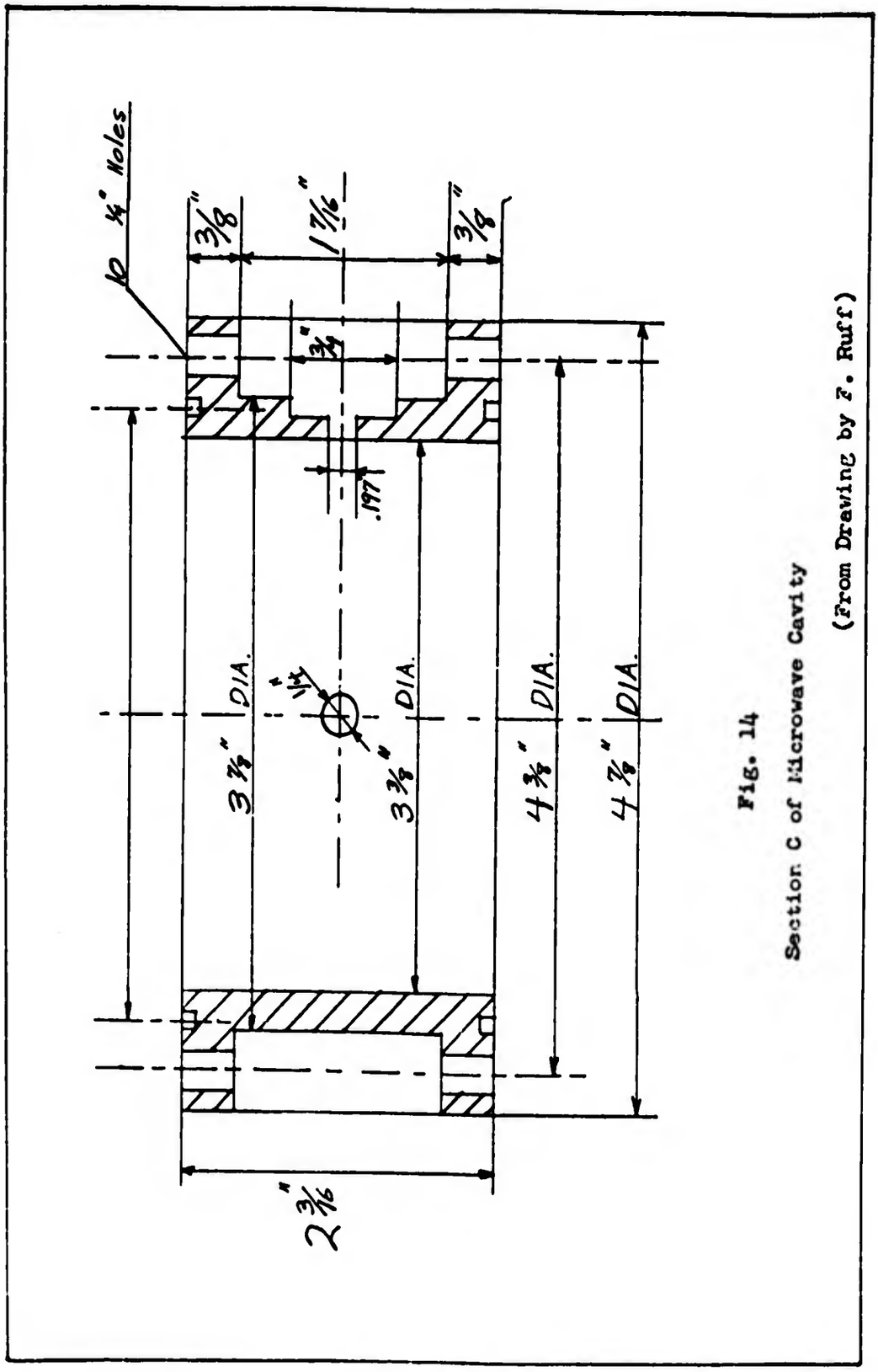

Fig. 14

Section C of Microwave Cavity

(From Drawing by F. Ruff)

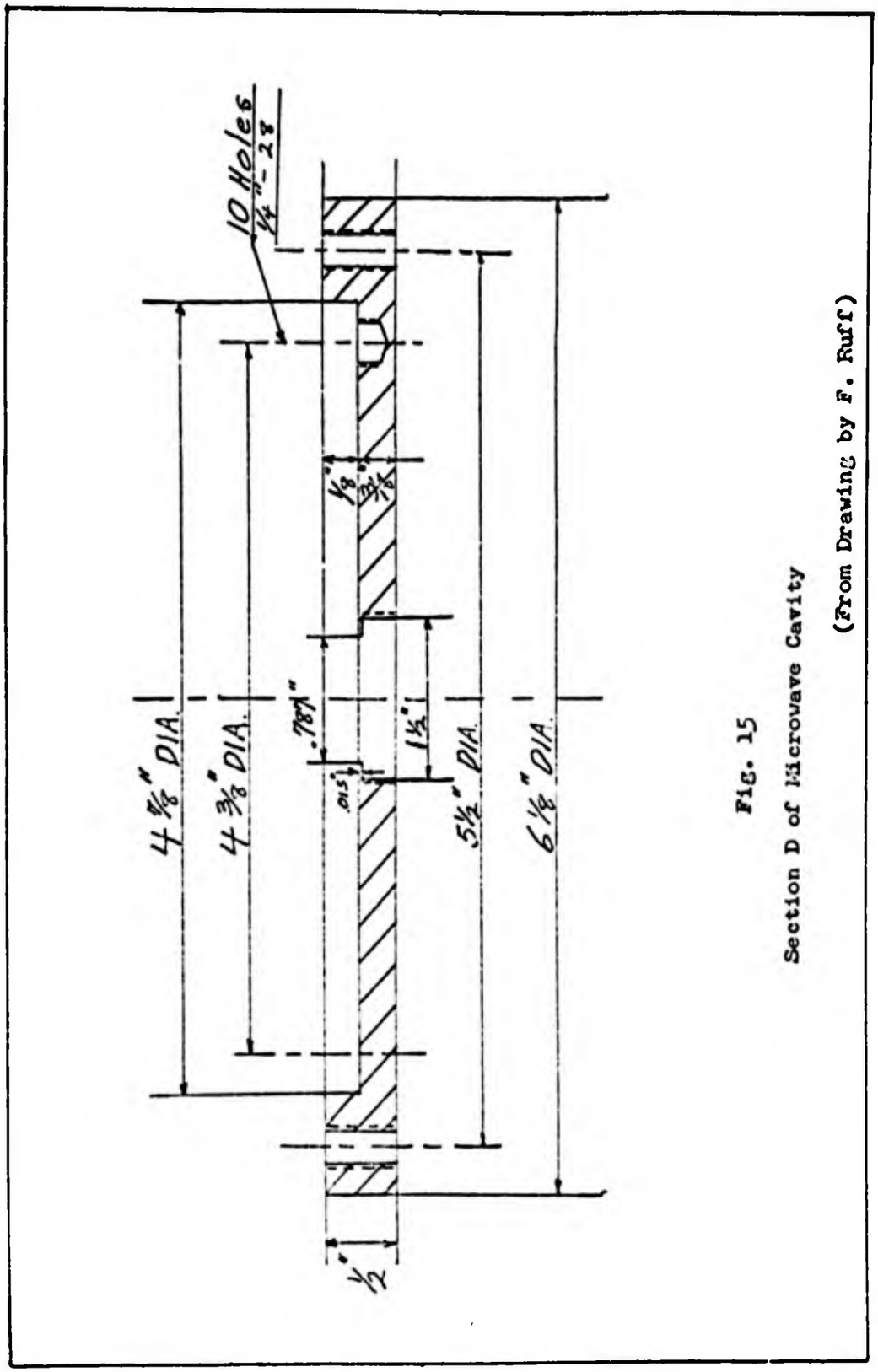

Fig. 15

Section D of Microwave Cavity

(From Drawing by F. Ruff)

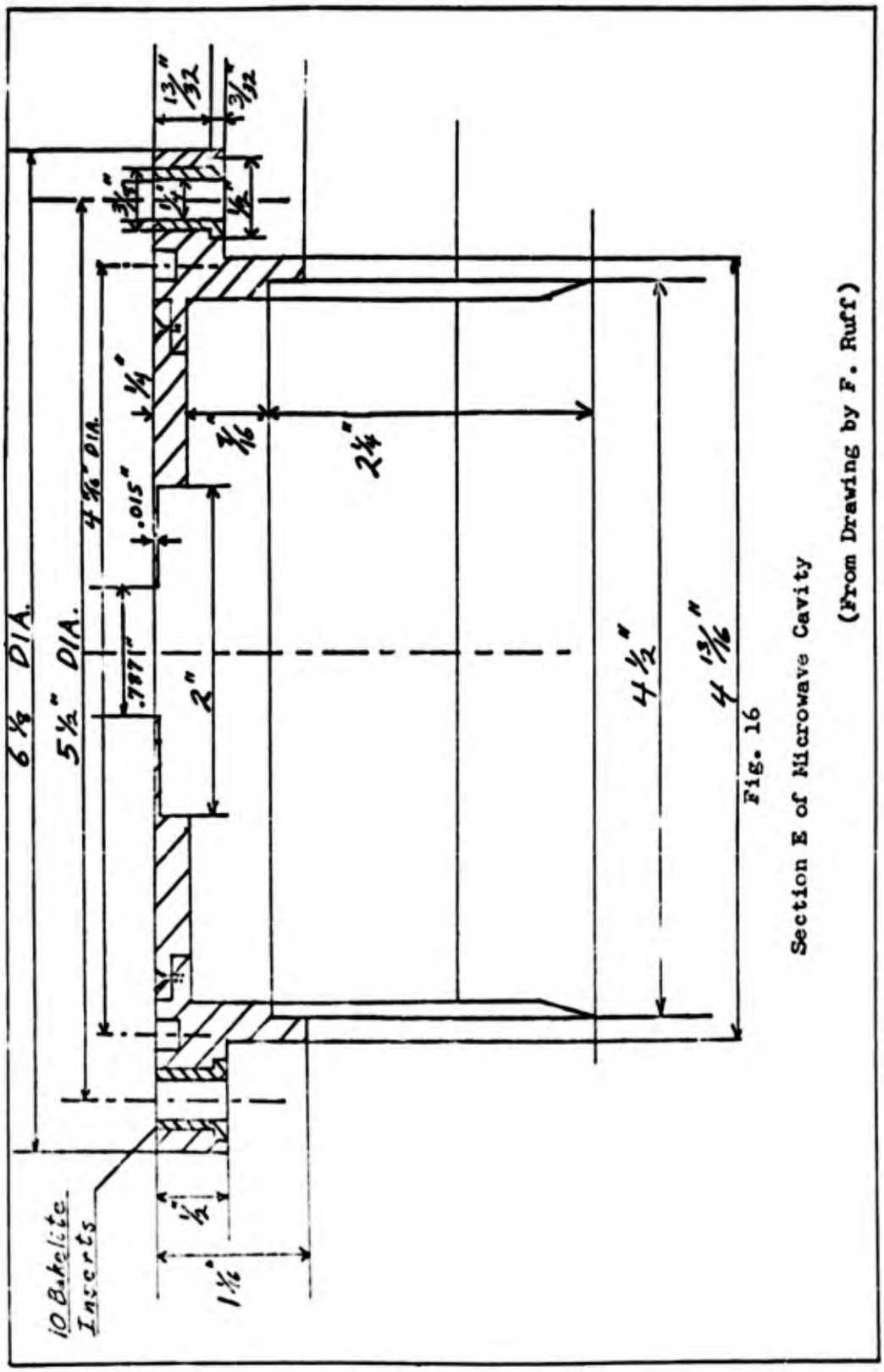

Section E of Microwave Cavity

(From Drawing by F. Ruff)

Fig. 16

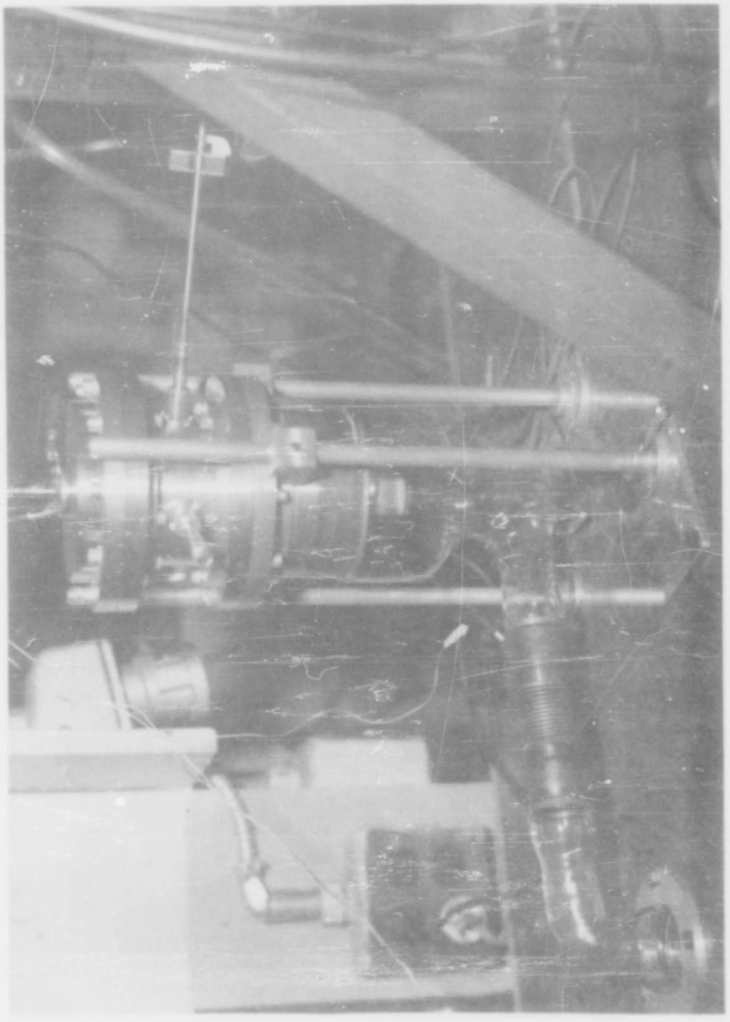

Fig. 17

Microwave Cavity and Plasma Tube

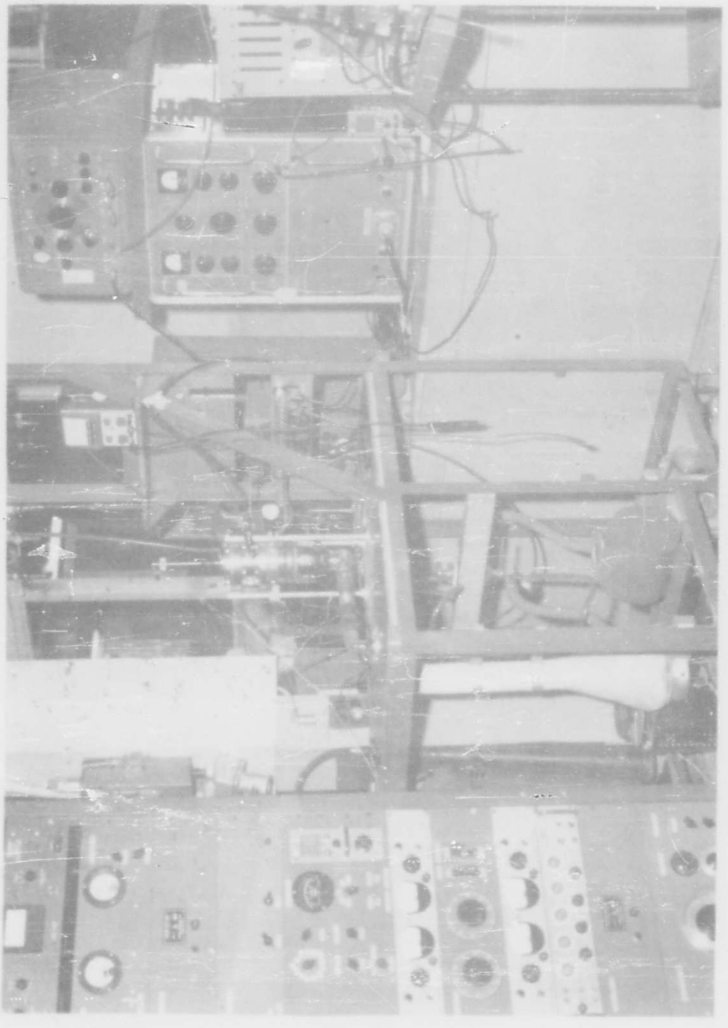

Fig. 18

Complete Experimental Apparatus

GNE/Phys/62-11

Vita

Robert R. Murfitt was born on [redacted] the son of Roscoe William and Evelyn [redacted] Murfitt. After graduation from [redacted], he attended Purdue University, Lafayette, Indiana. After graduation from Purdue University in 1956 with a Bachelor of Science Degree in Physics, he was commissioned as a Lieutenant in the USAF Reserve and attended pilot training at Spence Air Base, Georgia, and Vance Air Force Base, Oklahoma. His military assignment prior to his coming to the Institute of Technology was with the Military Air Transport Service at McGuire Air Force Base, New Jersey.

Permanent address: [redacted]

This thesis was typed by Miss Jean Doody.

UNCLASSIFIED